THE COMPLETE FAMILY OF ARNOUX–YOCCOZ SURFACES

JOSHUA P. BOWMAN

Abstract. The family of translation surfaces (X_g, ω_g) constructed by Arnoux and Yoccoz from self-similar interval exchange maps encompasses one example from each genus g greater than or equal to 3. We triangulate these surfaces and deduce general properties they share. The surfaces (X_g, ω_g) converge to a surface $(X_\infty, \omega_\infty)$ of infinite genus and finite area. We study the exchange on infinitely many intervals that arises from the vertical flow on $(X_\infty, \omega_\infty)$ and compute the affine group of $(X_\infty, \omega_\infty)$, which has an index 2 cyclic subgroup generated by a hyperbolic element.

Contents

1. Introduction

1.1. **From the golden ratio to the geometric series.** From our calculus courses, we know that the infinite geometric series $\frac{1}{2} + \frac{1}{4} + \frac{1}{8} + \cdots$ converges to 1. Indeed, using the summation formula $\sum_{k=1}^{\infty} x^k = x/(1-x)$, we find that $\frac{1}{2}$ is the unique solution to the equation $\sum_{k=1}^{\infty} x^k = 1$. From even earlier in our lives, perhaps, we recall that the equation $x + x^2 = 1$ has a unique positive solution, whose inverse is the golden ratio. The expression $x + x^2$ may be viewed as a partial geometric series, which can be extended to n terms: $x + \cdots + x^n$.

The positive solutions to the equations $x + \cdots + x^n = 1$ for $n \geq 3$ are instrumental in creating a certain family of measured foliations on surfaces, which was introduced by P. Arnoux and J.-C. Yoccoz in 1981 [AY]. In contemporary terminology, these measured foliations are the vertical foliations of certain translation surfaces. These surfaces were discovered in an attempt to provide examples of pseudo-Anosov homeomorphisms, which had been defined only a few years previously by W. Thurston in his classification of surface homeomorphisms [Th]. It was shown some time later (2005) by P. Hubert and E. Lanneau [HL] that the Arnoux–Yoccoz examples do not arise from the Thurston–Veech construction via compositions of multi-twists [Th, Ve]; in particular, their affine groups contain no parabolic elements.

Date: November 3, 2010.

In this paper, after providing some background on translation surfaces, we will present the surfaces constructed by Arnoux and Yoccoz and give explicit triangulations, then use these to prove certain properties common to all these surfaces. We will also see that the family can be extended to include the cases $n = 2$ and $n = \infty$. These extreme cases will turn out to be exceptional in their construction—the first corresponds to a singular surface (see the Appendix) and the second to a surface of infinite type (see §3)—but we hope that the self-similarity property that the golden ratio and the geometric series share with all of the other examples (see §2) will illuminate the entire sequence of surfaces for the reader.

1.2. **Background on translation surfaces.** There are two commonly accepted definitions for a "translation surface": either a surface with a translation atlas, or a Riemann surface with an abelian differential ω. These definitions are not quite equivalent. The former endows the surface with a Riemannian metric (given in a translation chart z by $|\mathrm{d}z|^2$) so that it is everywhere locally isometric to the Euclidean plane. The latter allows a discrete set of points on the surface to have neighborhoods isometric to "cone points" with respect to the metric $|\omega|^2$; these "singularities" of the metric occur at zeroes of ω and have angles that are integer multiples of 2π. This latter convention is necessary, for instance, in order to have compact translation surfaces of genus ≥ 2. Yet it is not hard to move from the complex-analytic definition to the Riemannian definition by simply "puncturing" the surface at the cone points. For convenience, then, we adopt the following convention.

Definition 1.1. A *translation surface* is a pair (X, ω), where X is a Riemann surface and $\omega \neq 0$ is a holomorphic 1-form on X.

Note that X is not assumed to be compact in the above definition.

Definition 1.2. Let (X, ω) be a translation surface. A homeomorphism $\varphi : X \to X$ is called *affine* if it is affine with respect to the canonical charts of ω. The group of affine homeomorphisms from X to itself is denoted $\mathrm{Aff}(X, \omega)$.

Any affine homeomorphism φ has a globally well-defined derivative $\operatorname{der}\varphi \in \mathrm{GL}_2(\mathbb{R})$; this is essentially because the group of translations is normal in the group of all affine bijections of $\mathbb{R}^2$. If (X, ω) has finite area, then necessarily any $\varphi \in \mathrm{Aff}(X, \omega)$ satisfies $\det(\operatorname{der}\varphi) = \pm 1$; in this case, the dynamical type of the map φ can be easily determined [Th, K, Ch]: let Tr denote the trace function.

- If $|\operatorname{Tr}\operatorname{der}\varphi| < 2$, then φ has finite order.
- If $|\operatorname{Tr}\operatorname{der}\varphi| = 2$, then (X, ω) decomposes into parallel cylinders such that on each cylinder some power of φ acts as a power of a Dehn twist.
- If $|\operatorname{Tr}\operatorname{der}\varphi| > 2$, then φ is pseudo-Anosov.

The importance of the group $\{\operatorname{der}\varphi \mid \varphi \in \mathrm{Aff}(X, \omega)\}$ for compact X was first observed by Veech. We make the following general definition [Ve, EG].

Definition 1.3. Let (X, ω) be a translation surface. The image of the derivative map $\operatorname{der} : \mathrm{Aff}(X, \omega) \to \mathrm{GL}_2(\mathbb{R})$ is called the *Veech group* of (X, ω) and is denoted $\Gamma(X, \omega)$.

A great deal of general theory about compact translation surfaces (and their moduli spaces) has been developed, by too many authors to name. Recently, several classes of non-compact translation surfaces and their Veech groups have been studied. Many of these are surfaces that cover compact surfaces and whose Veech groups are therefore contained in Veech groups of compact surfaces (e.g., [HHW, HLT]). Notable exceptions are a surface made from two infinite polygons inscribed in parabolas, which can be obtained as a limit of Veech's original examples [Hoo], and a family of "hyperelliptic" surfaces of finite area and infinite genus [Ch]. The surface we present in §3 combines certain features of these last two examples: it is a geometric limit of compact surfaces, and it has finite area. Future work on other such limits seems called for; at the end of this work, we discuss a possible direction for research on Veech groups of geometric limits of translation surfaces (Remark 4.12).

2. From intervals to triangles

2.1. **Pisot numbers and interval exchange maps.** In this section we review the algebraic numbers and interval exchange maps involved in the construction of the Arnoux–Yoccoz translation surfaces. Given any $g \geq 2$, the polynomial

$$x^g + x^{g-1} + \cdots + x - 1 \tag{1}$$

has a unique positive root, since its values at 0 and 1 are -1 and $g-1$, respectively, and its derivative is positive for all positive x. We denote the positive root of (1) simply as α, suppressing its dependence on g. Arnoux and Yoccoz showed that the inverse of α is a Pisot number, which means that α is in fact the only root of (1) that lies within the unit disk. Hubert and Lanneau remarked that, if g is even, then (1) has one negative root, and if g is odd, then α is the only real root. We add to these properties the following:

Lemma 2.1. *For each $g \geq 2$, the positive root α of* (1) *satisfies*

$$\frac{1}{2^{g+2}} < \alpha - \frac{1}{2} < \frac{1}{2^{g+1}}. \tag{2}$$

Proof. To obtain the lower bound, we claim that, when $r = 1/2 + 1/2^{g+2}$, the polynomial (1) evaluated at r is negative. This is equivalent to

$$\frac{1 - r^{g+1}}{1 - r} < 2, \qquad \text{or} \qquad \left(1 + \frac{1}{2^{g+1}}\right)^{g+1} > 1,$$

which is true for all $g \geq 2$. The upper bound is obtained similarly. □

Arnoux and Yoccoz [AY] introduced an interval exchange map based on the geometric properties of α. First, the unit interval is subdivided into g intervals of lengths α, α^2, ..., α^g. Each of these subintervals is divided in half, and the halves are exchanged within each subinterval. Finally the entire unit interval is divided into half, and these two halves are exchanged. We denote the total process f_g (see Figure 1). We will occasionally be interested in the behavior of f_g and its iterates on the endpoints of the subintervals, so for specificity we restrict the map to $[0, 1)$ and assume that the left endpoint of each piece is carried along. The key feature of f_g is its self-similarity:

Proposition 2.2 (Arnoux–Yoccoz)**.** *Let $\tilde{f}_g$ be the interval exchange map induced on $[0, \alpha)$ by the first return map of f_g. Then f_g is conjugate to $\tilde{f}_g$.*

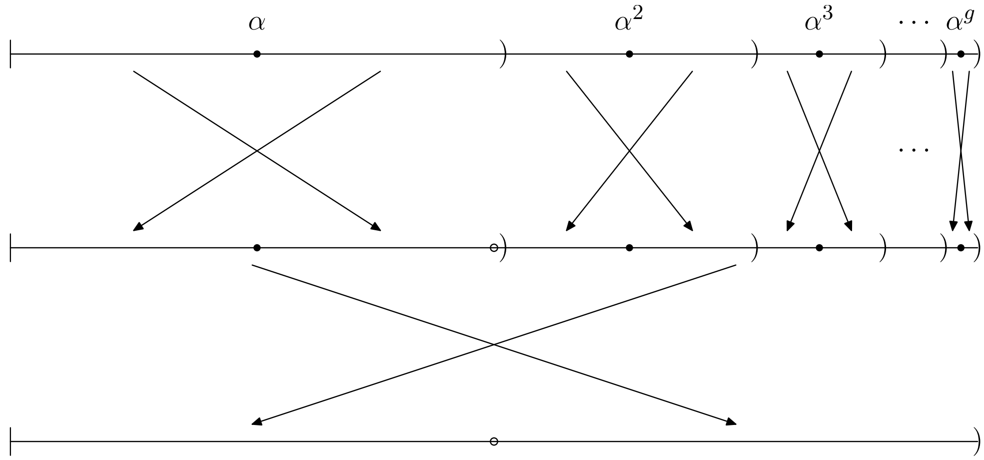

FIGURE 1. The interval exchange f_g as a composition of two involutions.

The proof uses an explicit piecewise affine map $h_g : [0,1) \to [0,\alpha)$, defined as follows:

$$h_g(x) = \begin{cases} \alpha x + \frac{\alpha+\alpha^{g+1}}{2}, & x \in \left[0, \frac{1-\alpha^g}{2}\right) \\ \alpha x - \frac{\alpha-\alpha^{g+1}}{2}, & x \in \left[\frac{1-\alpha^g}{2}, 1\right) \end{cases}$$

which satisfies $f_g = h_g^{-1} \circ \tilde{f}_g \circ h_g$. In §3, we will show similar kinds of results for certain exchanges on infinitely many subintervals.

In their original paper, citing work of G. Levitt, Arnoux and Yoccoz state that, for a given interval exchange map:

> *. . . on peut construire une suspension canonique, et l'on sait que toute suspension possédant les mêmes singularités (en type et en nombre) que cette suspension canonique lui est homéomorphe par un homéomorphisme préservant la mesure transverse du feuilletage.*

(The "canonical suspension" is a measured foliation on a compact surface together with a closed curve transverse to the foliation on which the first return map of the foliation induces the given interval exchange map.) They then use this result and the self-similarity of f_g to demonstrate the existence of a pseudo-Anosov homeomorphism ψ_g on a surface of genus g such that the expansion constant of ψ_g is $1/\alpha$. In a separate paper [Ar], Arnoux gives an explicit description of the canonical suspension of f_3 and illustrates ψ_3. In §§2.2–2.3 we will present the generalization of Arnoux's construction to all genera and exploit these presentations to make further conclusions about the Arnoux–Yoccoz surfaces.

2.2. **Steps and slits.** Fix $g \geq 3$. In this section, we will present the genus g Arnoux–Yoccoz surface (X_g, ω_g) by generalizing Arnoux's presentation of (X_3, ω_3). Starting with a unit square, we carve out a "staircase" in the upper right-hand corner, with the widths of the steps, from left to right, given by α, α^2, …, α^g, and the distances between the steps, going down, given by α^g, α^{g-1}, …, α. We further slit this square along several vertical segments σ_1, σ_2, …, σ_g. The slits are made starting along the bottom edge of the square at points whose x-coordinates are images by f_g of the left-hand endpoints of the intervals

$\left[\frac{\alpha-\alpha^i}{1-\alpha}, \frac{\alpha-\alpha^{i+1}}{1-\alpha}\right)$, for $1 \le i \le g$. (N.B.: the lower endpoints of the slits are not singularities on the resulting surface, following the rest of the construction below.)

Now we wish to provide appropriate gluings for the surface to have an affine self-map. These identifications are as follows:

- The tops of the steps are glued to the bottom of the unit square according to the interval exchange f_g.
- The vertical edge of the bottommost step, having length α, is identified with the bottom portion of the leftmost vertical edge.
- The remaining top portion of the leftmost edge of the square, having length $1-\alpha$, is identified with the bottom portion to the left of σ_1.
- The remaining top portion to the left of σ_1 is identified with the right side of σ_g.
- The vertical edge of the step having height α^i $(2 \le i \le g)$ is identified with the bottom portion to the right of the segment σ_{i-1}.
- The remaining top portion to the right of each segment σ_i $(1 \le i \le g-1)$ is identified with the left side of the segment σ_{i+1}.

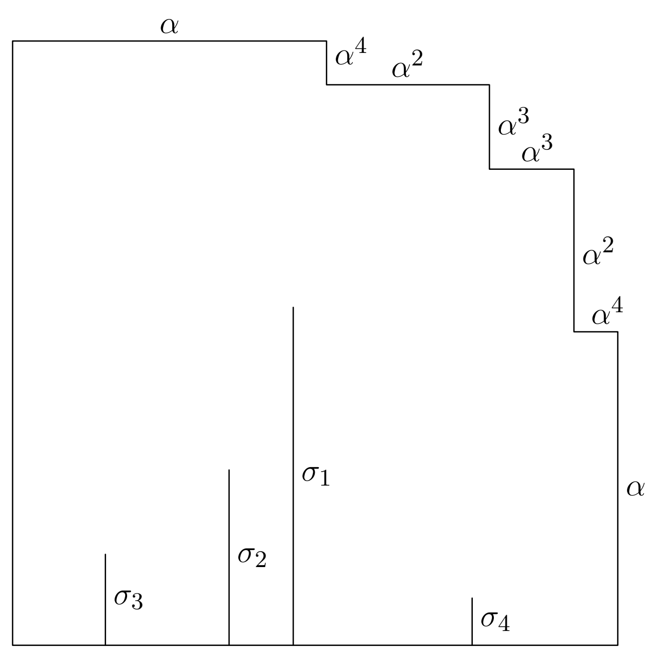

FIGURE 2. The steps and slits for the genus 4 Arnoux–Yoccoz surface.

There is a one real-parameter family of surfaces that satisfy the gluings given above; the easiest parameter to vary is $|\sigma_g|$. We want to single out a value for this parameter so that the surface admits a pseudo-Anosov affine map. The required condition is described by the equation $\alpha(1+|\sigma_g|) = (1-\alpha) + |\sigma_g|$, which says that the length of σ_1 is α times the sum of the length of σ_g and the length of the left edge of the square (i.e., 1). Solving this equation, we find $|\sigma_g| = (2\alpha-1)/(1-\alpha)$, which determines the lengths of the remaining slits.

The pseudo-Anosov homeomorphism $\psi_g : X_g \to X_g$ expands the horizontal foliation of ω_g by a factor of $1/\alpha$ and contracts the vertical foliation by a factor of α. It permutes the vertical segments in a predictable manner: for each i from 1 to $g-1$, ψ_g sends σ_i to σ_{i+1}, and also sends the union of σ_g with the left-hand edge of the initial square to σ_1. The step of height α^i is also sent to the step of height α^{i+1} ($1 \le i \le g-1$).

2.3. **Triangulation of** (X_g, ω_g)**.** Let g be as in §2.2. Now we give an alternate construction of the surface (X_g, ω_g) from $4g$ triangles. Begin with the points $P_0, \ldots, P_g, Q_0, \ldots, Q_g$ in $\mathbb{R}^2$, chosen as follows (see Figure 3):

$$P_0 = \left(\frac{1-\alpha^g}{2}, \frac{\alpha^2}{1-\alpha}\right), \qquad Q_0 = \left(-\frac{\alpha^g}{2}, \alpha\right),$$
$$P_1 = \left(-\frac{\alpha^{g-1}+\alpha^g}{2}, \frac{\alpha-\alpha^2+\alpha^3}{1-\alpha}\right),$$
$$P_g = \left(1+\frac{\alpha-\alpha^g}{2}, \frac{3\alpha-1-\alpha^2}{1-\alpha}\right),$$
$$P_i = \left(\frac{\alpha-\alpha^i}{1-\alpha}, \frac{\alpha}{1-\alpha}\right) \qquad \text{for } i = 2, \ldots, g-1,$$
$$Q_i = \left(\frac{2\alpha-\alpha^i-\alpha^{i+1}}{2(1-\alpha)}, \frac{\alpha-\alpha^{g-i+2}}{1-\alpha}\right) \qquad \text{for } i = 1, \ldots, g.$$

For $i = 1, \ldots, g$, set $T_i = P_0Q_iQ_{i-1}$ and $T_{g+i} = P_iQ_{i-1}Q_i$. For $i = 1, \ldots, 2g$, let T_i' be the reflection of T_i in the horizontal axis. Glue the T_is along their common boundaries, and likewise for the T_i's. Then each remaining "free" edge is a translation of another; we glue each such pair of edges:

- P_0Q_0 is paired with $P_0'Q_g'$, and $P_0'Q_0'$ is paired with P_0Q_g.
- P_1Q_1 is paired with $P_g'Q_{g-1}'$, and $P_1'Q_1'$ is paired with P_gQ_{g-1}.
- P_1Q_0 is paired with $P_{g-1}Q_{g-1}$, and $P_1'Q_0'$ is paired with $P_{g-1}'Q_{g-1}'$.
- P_gQ_g is paired with Q_1P_2, and $P_g'Q_g'$ is paired with $Q_1'P_2'$.
- For $i = 2, \ldots, g-2$, P_iQ_i is paired with $Q_i'P_{i+1}'$ and $P_i'Q_i'$ is paired with Q_iP_{i+1}.

All of the P_is and Q_i's are identified to become a cone point, and likewise for all of the Q_is and P_i's. The resulting surface therefore has genus g and lies in the stratum $\mathcal{H}(g-1, g-1)$.

One can verify the following result directly by checking that the surface we have constructed from triangles is isometric to the staircase presentation (cf. Figures 3 and 4).

Proposition 2.3. *The T_is and T_i's induce a triangulation of (X_g, ω_g).*

By "triangulation" we mean the structure of a Δ-complex, in the sense of Hatcher [Ha]; we also require that the set of vertices contain the cone points and the 1-cells be geodesic.

Corollary 2.4. $\mathrm{Aff}(X_g, \omega_g)$ *contains a fixed-point free, orientation-reversing involution ρ_g, which commutes with ψ_g, and whose derivative is reflection in the x-axis.*

The existence of this symmetry occurs for a completely general reason: f_g is conjugate to its inverse by the following "rotation" of the unit interval:

$$r(x) = \begin{cases} x + \frac{1}{2}, & x \in [0, \frac{1}{2}) \\ x - \frac{1}{2}, & x \in [\frac{1}{2}, 1) \end{cases}$$

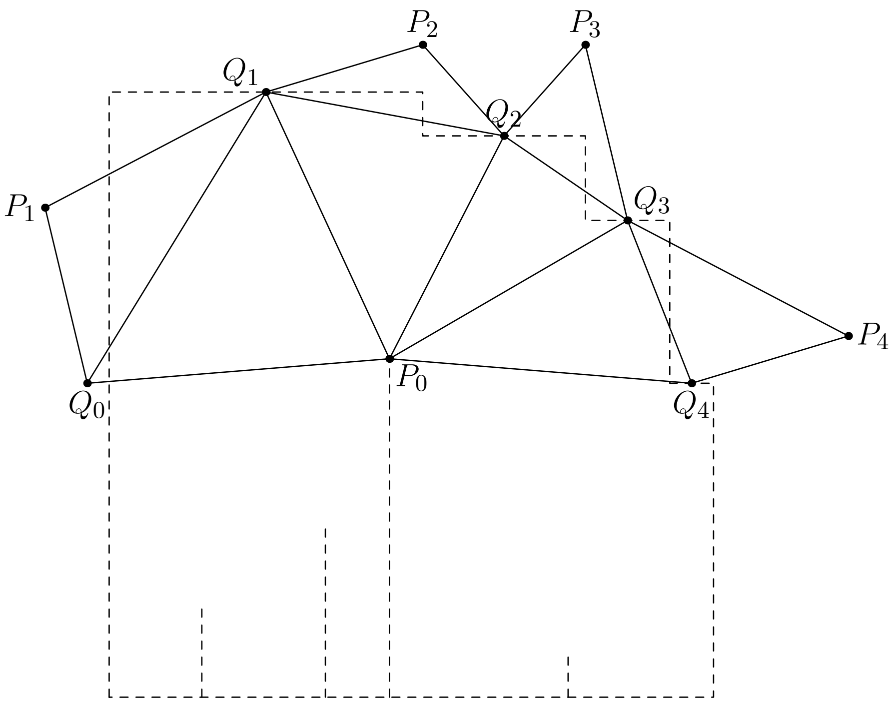

FIGURE 3. The points $P_0, \ldots, P_4, Q_0, \ldots, Q_4$ relative to (X_4, ω_4)'s staircase.

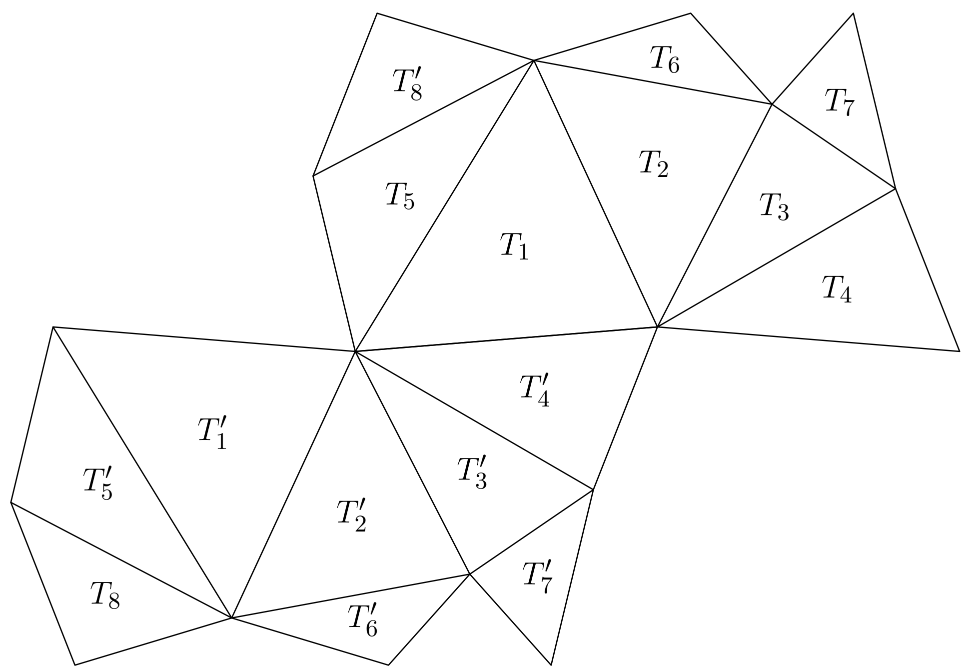

FIGURE 4. A triangulation of (X_4, ω_4).

By the reasoning invoked in §2.1, the surface obtained from (X_g, ω_g) by applying complex conjugation to the charts of ω_g (which is a suspension of f_g^{-1}, and therefore of f_g) is translation equivalent to (X_g, ω_g) itself, which yields the existence of ρ_g.

Corollary 2.5. *The compact non-orientable surface of Euler characteristic $1-g$ admits a pseudo-Anosov homeomorphism whose invariant foliations have one singular point and whose expansion constant has degree g.*

This corollary generalizes a result from [AY], in which it is shown that (X_3,ω_3) can also be constructed by lifting a measured foliation on $\mathbb{RP}^2$ first to the non-orientable surface of Euler characteristic -2 and then to genus 3.

Corollary 2.6. *If $g \geq 4$, then X_g is not hyperelliptic.*

Proof. Every abelian differential on a hyperelliptic surface is odd with respect to the hyperelliptic involution. If, for some $g \geq 4$, X_g were hyperelliptic, then there would have to be an isometry of (X_g,ω_g) with derivative $-\mathrm{id}$. Such an isometry would, for instance, have to send the segment $P_{g-1}Q_{g-1}$ to a parallel segment of the same length. This segment cannot be preserved by the isometry, because it would have to be rotated around its midpoint—but Q_{g-2} (which is opposite $P_{g-1}Q_{g-1}$ in the triangle T_{2g-1}) has no potential image on the other side of P_1Q_0 (which is identified with $P_{g-1}Q_{g-1}$). It is easily checked that no other saddle connections on (X_g,ω_g) are parallel to $P_{g-1}Q_{g-1}$ and have the same length. Hence no isometry with derivative $-\mathrm{id}$ exists. □

Remark 2.7. The surface X_3 is well-known to be hyperelliptic. (In [Bo], Weierstrass equations are given for two surfaces affinely equivalent to (X_3,ω_3); see also [HLM].) The obstruction described in the proof of Corollary 2.6 does not occur in genus 3, because the segment P_2Q_2 does in fact have another saddle connection with the same length and direction, namely, P_0Q_1. The hyperelliptic involution of X_3 exchanges each T_i and T_{g+i} by rotating around the midpoint of their common edge.

3. A limit surface: (X_∞,ω_∞)

Lemma 2.1 implies that each triangle that appears in the construction of some (X_g,ω_g) has a "limiting position"; from these we can construct a "limit surface" of infinite genus. See Figure 5 for the definition of this surface. To be precise, we obtain a non-compact translation surface (X_∞,ω_∞), where X_∞ has infinite genus, whose metric completion is the one-point compactification of X_∞. Here, as usual, ω_∞ is the 1-form induced on the quotient by $\mathrm{d}z$ in the plane. In a sense, the two cone points of the (X_g,ω_g), $g<\infty$, have "collapsed" into each other, leaving an essential singularity at which all of the "curvature" of the space (X_∞,ω_∞) is concentrated. We shall briefly address in §4 the behavior of (X_∞,ω_∞) near this singular point. A *critical trajectory* of (X_∞,ω_∞) is a geodesic trajectory that leaves every compact subset of X_∞. A *saddle connection* of (X_∞,ω_∞) is a geodesic trajectory (of finite length) that leaves every compact subset of X_∞ in both directions.

Theorem 3.1. *X_∞ is a Riemann surface of infinite genus with one end, and ω_∞ is an abelian differential of finite area on X_∞ without zeroes on X_∞.* $\mathrm{Aff}(X_\infty,\omega_\infty)$ *includes an orientation-reversing isometric involution ρ_∞ without fixed points on X_∞ and a pseudo-Anosov homeomorphism ψ_∞ with expansion constant* 2. *These two elements commute.*

Proof. (In this paragraph, we follow the method of proof used by R. Chamanara in [Ch].) That X_∞ is a Riemann surface is evident, as are the claims about ω_∞. The fact that X_∞ has

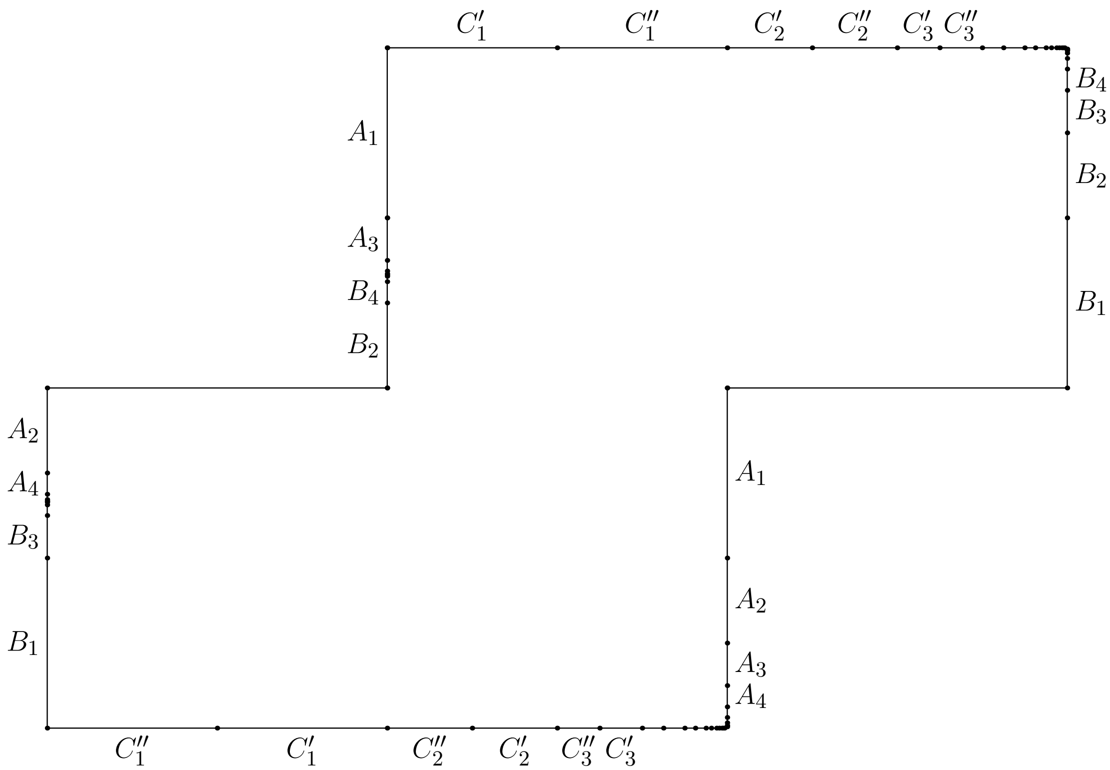

FIGURE 5. The surface $(X_\infty, \omega_\infty)$. Each pair of edges with the same label is identified by translation, as is the remaining pair of unlabeled edges. The length of each A_n, B_n, C_n', or C_n'' is $1/2^{n+1}$.

infinite genus can be deduced from the existence of a set of pairwise non-homotopic simple closed curves $\{\gamma_n', \gamma_n''\}_{n\in\mathbb{N}}$, where γ_n' (respectively, γ_n'') connects the midpoints of the edges labelled C_n' (respectively, C_n''), and each γ_n' intersects only γ_n'' (and vice versa). To show that X_∞ has only one topological end, we construct a sequence of compact subsurfaces with boundary. Let K_g be the complement of the union of the open squares having side length $1/2^{g+1}$ and centered at the endpoints of the segments A_n, B_n, C_n', C_n''. These K_g satisfy $K_g \subset K_{g+1}$ and $\bigcup K_g = X_\infty$, and the complement of each K_g has one component. Therefore by definition X_∞ has one topological end.

The orientation-reversing affine map ρ_∞ is visible in Figure 5 as a glide-reflection in a horizontal axis with translation length $1/2$. It sends the interior of the upper rectangle to the interior of the lower rectangle, each edge labeled A_n to an edge labeled B_n, and each edge labeled C_n' to an edge labeled C_n''. Therefore it has no fixed points.

Now we demonstrate the pseudo-Anosov affine map ψ_∞. Let R be the central rectangle in Figure 5, and let S_1 and S_2 be the squares in the lower left and upper right, respectively. Expand R horizontally by a factor of 2, and contract R vertically by a factor of $1/2$ to obtain $\psi_\infty(R)$. Do the same with the rectangle R' which is the union of S_1 and S_2 (the top edge of S_1 is glued to the bottom edge of S_2) to obtain $\psi_\infty(R')$. Take $\psi_\infty(R)$ and lay it over S_1 and the lower half of R, and lay $\psi_\infty(R')$ over S_2 and the top half of R. This affine map is compatible with all identifications. That ψ_∞ and ρ_∞ commute may be checked directly. $\square$

Remark 3.2. The pseudo-Anosov map $\psi_\infty : X_\infty \to X_\infty$ is a variant of the well-studied baker map, and thus $(X_\infty, \omega_\infty)$ is an alternate infinite-genus realization of this map, which was demonstrated on a "hyperelliptic" infinite-genus surface by Chamanara–Gardiner–Lakic [CGL]. The topological type of X_∞ is that of a "Loch Ness monster" and is therefore related to the surfaces described in [PSV], although the flat structure of ω_∞ does not fall into the class of surfaces studied there.

Let us make precise the notion of $(X_\infty, \omega_\infty)$ as a "limit" of (X_g, ω_g). We establish canonical piecewise-affine embeddings $\iota_g : K_g \to X_g$, where the K_g are the subsurfaces defined in the proof of Theorem 3.1, in such a way that $\iota_g^* |\omega_g|$ converges to $|\omega_\infty|$ on compact subsets of X_∞ as $g \to \infty$. (Here $|\omega_n|$ indicates the metric induced on X_n by ω_n, $3 \le n \le \infty$.) In fact, each ι_g will be defined on an open set U_g containing K_g and dense in X_∞.

For each $3 \le g < \infty$, let U_g be the surface obtained from Figure 5 by making all identifications up through index $\lfloor g/2 \rfloor$ for the A_is and B_is, and all identifications up through index $\lfloor (g-1)/2 \rfloor$ for the C_i's and the C_i''s. (Here and in what follows $x \mapsto \lfloor x \rfloor$ denotes the "floor" function.) Retract the union of the triangles

$$\left\{ \left(\frac{1}{2}, \frac{1}{2}\right), \left(1, \frac{2^{\lfloor g/2 \rfloor} - 1}{2^{\lfloor g/2 \rfloor}}\right), (1,1) \right\} \quad \text{and} \quad \left\{ \left(\frac{1}{2}, \frac{1}{2}\right), (1,1), \left(\frac{2^{\lfloor (g-1)/2 \rfloor} - 1}{2^{\lfloor (g-1)/2 \rfloor}}, 1\right) \right\}$$

onto the triangle $\{(1/2, 1/2), (1, 1 - 1/2^{\lfloor g/2 \rfloor}), (1 - 1/2^{\lfloor (g-1)/2 \rfloor}, 1)\}$ by a homeomorphism, affine on each of the original triangles. Now a surface of genus g with two punctures can be created directly by identifying the "free" edge of this triangle with one of the "free" segments on the leftmost edges of the polygon. (N.B.: at this stage, this final identification is not by a translation, but it can be chosen to be affine.)

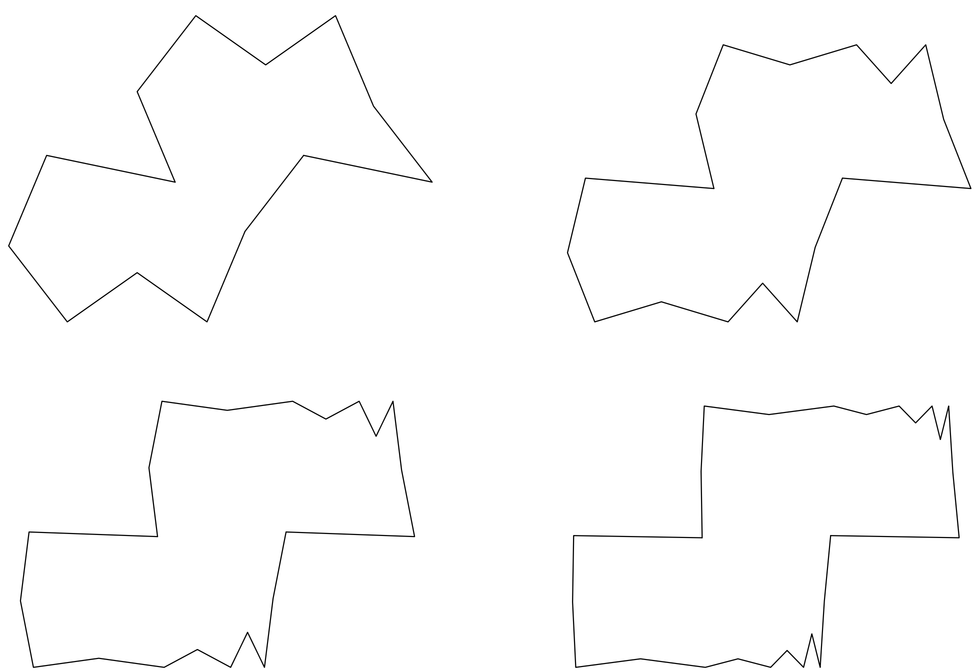

FIGURE 6. Outlines of the surfaces (X_g, ω_g) for $g = 3, 4, 5, 6$.

Figure 6 shows the outlines of the first few surfaces in the sequence (X_g, ω_g). By adjusting the positions of the triangles in the upper right and upper left corners (e.g., removing the triangles labelled $T_{2g-\lfloor g/2 \rfloor}$ through T_{2g}, in addition to their mirror images, and regluing them along their longest edges in the appropriate location—cf. Figure 4 and the description in §2.2), one finds that there is a piecewise-affine map ι_g carrying U_g to X_g. Moreover, because $U_{g-1} \subset U_g$, ι_g restricts to an embedding of U_{g-1}, as well.

Theorem 3.3. *The metrics $\iota_g^* |\omega_g|$ converge to $|\omega_\infty|$ uniformly on compact subsets of X_∞.*

Proof. Any compact $K \subset X_\infty$ is contained in some U_g. For any pair of points $P', P'' \in K$, the ratio of the distance from P' to P'' in each of the metrics $\iota_g^* |\omega_g|$ and $|\omega_\infty|$ is bounded by the quasi-conformal constants and the Jacobian determinants of the maps ι_g, which are uniformly bounded over all of K. As these constants approach 1, so do the ratios of lengths over K, uniformly. □

4. The affine group of $(X_\infty, \omega_\infty)$

In this section we will explore some of the geometry and dynamics of $(X_\infty, \omega_\infty)$, culminating in a proof of the following:

Theorem 4.1. $\mathrm{Aff}(X_\infty, \omega_\infty) \cong \mathbb{Z} \times \mathbb{Z}/2\mathbb{Z}$ *is generated by ψ_∞ and ρ_∞.*

4.1. **An exchange on infinitely many intervals.** Let us revise our definition of "interval exchange map" to include injective maps from an interval to itself that are upper semicontinuous piecewise isometries. (This keeps with the "continuous at left endpoints" convention, although we may lose the property of bijectivity, as we shall see in a later example.) Then the vertical foliation of $(X_\infty, \omega_\infty)$ induces an interval exchange map $f_\infty : [1, 0) \to [1, 0)$, which can also be defined by a two-step process: first, swap the two halves of each interval $[\frac{2^n-1}{2^n}, \frac{2^{n+1}-1}{2^{n+1}})$, for $0 \le n < \infty$, then swap $[1, 1/2)$ with $[1/2, 1)$; cf. §2.1.

We can encode f_∞ symbolically as follows: if we do not allow the binary expansion of a number to terminate with only 1s, then each number in $[0, 1)$ has a unique binary expansion. Use these to identify $[0, 1)$ with the set $\mathfrak{B} \subset (\mathbb{F}_2)^{\mathbb{N}}$ consisting of sequences that do not terminate with only 1s. Given a sequence $a = a_0 a_1 a_2 \cdots$, we obtain $f_\infty(a)$ as follows:

(1) find the first $i \in \mathbb{N}$ such that $a_i = 0$, and replace a_{i+1} with $a_{i+1} + 1$;
(2) replace a_0 with $a_0 + 1$.

The inverse map f_∞^{-1} simply reverses these two steps. Both f_∞ and f_∞^{-1} are bijections. We remark that the first return map of f_∞ on either $[0, 1/2)$ or $[1/2, 1)$ is simply the restriction of f_∞^2 to the respective interval.

To aid our study at this point, we use the map r defined in §2.2 along with the following:

$$h'(x) = \frac{x}{2}, \qquad h''(x) = (r \circ h')(x) = \frac{x}{2} + \frac{1}{2},$$

$$h_\infty(x) = (h' \circ r)(x) = \begin{cases} \frac{1}{2}\left(x + \frac{1}{2}\right), & x \in [0, \frac{1}{2}) \\ \frac{1}{2}\left(x - \frac{1}{2}\right), & x \in [\frac{1}{2}, 1) \end{cases}$$

In terms of binary expansions, we can describe the effects of these functions on a sequence $a \in \mathfrak{B}$ as follows:

- r replaces a_0 with $a_0 + 1$;
- h' appends a 0 to the beginning of the sequence;
- h'' appends a 1 to the beginning of the sequence;
- h_∞ replaces a_0 with a_0+1 and appends a 0 to the beginning of the sequence.

The formalism of encoding these maps to act on infinite binary sequences makes immediate the following result.

Lemma 4.2. *Let f_∞, r, h', h'', and h_∞ act on $\mathfrak{B}$ as above. Then:*

- *r conjugates f_∞ to f_∞^{-1}.*
- *h' conjugates $f_\infty^2|_{[0,1/2)}$ to f_∞^{-1}.*
- *h'' conjugates $f_\infty^2|_{[1/2,1)}$ to f_∞.*
- *h_∞ conjugates $f_\infty^2|_{[0,1/2)}$ to f_∞.*

Proof. We will prove the second claim. It is equivalent to show that $f_\infty^2 h' f_\infty = h'$. Let $a = a_0a_1a_2\cdots$ be a sequence in $\mathfrak{B}$, and let $i_0 \geq 0$ be the first value for which $a_{i_0} = 0$. Then $(h'f_\infty(a))_0 = 0$, $(h'f_\infty(a))_1 = a_0+1$, $(h'f_\infty(a))_{i_0+2} = a_{i_0+1}+1$, and $(h'f_\infty(a))_{i+1} = a_i$ for all other i. Applying f_∞ to $h'f_\infty(a)$ results in $(1, a_0, \ldots, a_{i_0-1}, 0, a_{i_0+1}+1, a_{i_0+2}, \ldots)$. Now i_0+1 is the first index i such that $(f_\infty h' f_\infty a)_i = 0$. Applying f_∞ again replaces $(f_\infty h' f_\infty a)_{i_0+2}$ with a_{i+1} and changes the leading 1 to a 0, so that $f_\infty^2 h' f_\infty(a) = h'(a)$.

The proofs of the other claims are similar; in fact, the first claim is trivial, while the latter two claims follow from the first two. $\square$

Remark 4.3. As a caveat regarding exchanges of infinitely many intervals, we describe the interval exchange F_∞ induced on a vertical segment by the horizontal foliation. We use the horizontal flow in the positive x-direction, in which case F_∞ has the following effect on $\mathfrak{B}$: for each sequence a,

(1) find the least $i > 0$ such that $a_i \neq a_0$;
(2) replace a_{i-1-2j} with $a_{i-1-2j}+1$ for all $0 \leq j \leq \lfloor i/2 \rfloor$.

Note that this algorithm fails to define F_∞ on the zero sequence $\bar{0}$; we will see momentarily that $1/3$ does not have a preimage by F_∞, and so we can define $F_\infty(0) = 1/3$ without compromising the injectivity or semicontinuity of F_∞. The inverse F_∞^{-1} acts on $\mathfrak{B}$ as follows: for each sequence a,

(1) find the least $i > 0$ such that $a_i = a_{i-1}$;
(2) replace a_{i-1-2j} with $a_{i-1-2j}+1$ for all $0 \leq j \leq \lfloor i/2 \rfloor$.

This algorithm fails for *two* points in $\mathfrak{B}$, namely $\overline{01} = 1/3$ and $\overline{10} = 2/3$; these have no pre-images by F_∞. Hence we can "fix" F_∞ by defining $F_\infty(0)$ to be either $1/3$ or $2/3$, but the choice is arbitrary. In either case, F_∞ will still not have all of $\mathfrak{B}$ as its image. The special role of $1/3$ and $2/3$ will be useful to keep in mind (see the proof of Lemma 4.10).

Let $\mathfrak{D} \subset [0,1)$ denote the set of dyadic rationals in $[0,1)$—that is, the set of rational numbers of the form $n/2^m$ for some $n, m \in \mathbb{Z}$. $\mathfrak{D}$ sits inside $\mathfrak{B}$ as the set of sequences that are eventually 0. For each $x \in [0,1)$, let $\mathcal{O}^\pm(x)$ be the orbit of x under $f_\infty^{\pm 1}$.

Lemma 4.4. $\mathfrak{D} = \mathcal{O}^\pm(0) \sqcup \mathcal{O}^\pm(1/2)$.

A more complete way to state this result is that the union of the forward and backward orbits of a sequence $a \in \mathfrak{D}$ is entirely determined by the parity of the number of 1s in the sequence a. We call $\mathrm{TM}(a) = \sum a_i \in \mathbb{F}_2$ the *Thue–Morse function*: for any particular $a \in \mathfrak{D}$, this sum has finitely many terms, and $\mathrm{TM}(a)$ is invariant under f_∞ because two digits are changed from a to $f_\infty(a)$. We also define the *index of* a to be the smallest natural number $\mathrm{Ind}(a) \in \mathbb{N}$ such that $a_i = 0$ for all $i > \mathrm{Ind}(a)$. (Recall that our sequences in $\mathfrak{B}$ start with a_0, and so $\mathrm{Ind}(\bar{0}) = \mathrm{Ind}(1\bar{0}) = 0$.) We will show that the following table determines which orbit contains $a \in \mathfrak{D} - \{\bar{0}, 1\bar{0}\}$:

(3)

		TM(a) = 0	TM(a) = 1
Ind(a)	even	$\mathcal{O}^-(0)$	$\mathcal{O}^+(1/2)$
	odd	$\mathcal{O}^+(0)$	$\mathcal{O}^-(1/2)$

One consequence of the proof will be a quick algorithm for computing the exact value of $n \in \mathbb{Z}$ such that $f_\infty^n(0) = a$ or $f_\infty^n(1/2) = a$.

Proof of Lemma 4.4. Let H be the semigroup of functions $\mathfrak{B} \to \mathfrak{B}$ consisting of words in h' and h''. The map from H to $\mathfrak{B}$ defined by $w \mapsto w(\bar{0})$ induces a set-theoretic bijection between $\mathfrak{D}$ and the quotient of H by the relation $w \sim wh'$. Throughout the proof, we will use the equivalence $\mathfrak{D} \leftrightarrow H/\sim$, by which $(a_0, a_1, \ldots, a_{\mathrm{Ind}(a)}, 0, \ldots)$ corresponds to the equivalence class of $\eta_0\eta_1 \cdots \eta_{\mathrm{Ind}(a)}$, with

$$\eta_i = \begin{cases} h' & \text{if } a_i = 0 \\ h'' & \text{if } a_i = 1 \end{cases}.$$

In particular, $\eta_{\mathrm{Ind(a)}} = h''$ if $\mathrm{Ind}(a) \geq 1$.

Let $a \in \mathfrak{D}$. We proceed by induction on $\mathrm{Ind}(a)$. Direct computation shows that

$$h''h''(\bar{0}) = f_\infty h'(\bar{0}) = f_\infty(\bar{0}) \qquad \text{and} \qquad h'h''(\bar{0}) = f_\infty^{-1}h''(\bar{0}) = f_\infty^{-1}(1\bar{0}),$$

and therefore if $\mathrm{Ind}(a) = 1$, a is in the union of the orbits of $\bar{0}$ and $1\bar{0}$. Now suppose $\mathrm{Ind}(a) \geq 2$, and let $w = \eta_0\eta_1 \cdots \eta_{\mathrm{Ind}(a)-1}h''$ be the corresponding word in H. Using the above computations, we can rewrite the effect of w on $\bar{0}$ in the following way:

$$w(\bar{0}) = \begin{cases} \eta_0\eta_1 \cdots \eta_{\mathrm{Ind}(a)-2} f_\infty h'(\bar{0}) & \text{if } \eta_{\mathrm{Ind}(a)-1} = h'' \\ \eta_0\eta_1 \cdots \eta_{\mathrm{Ind}(a)-2} f_\infty^{-1} h''(\bar{0}) & \text{if } \eta_{\mathrm{Ind}(a)-1} = h' \end{cases}.$$

From Lemma 4.2, we have

$$f_\infty^2 h' = h' f_\infty^{-1} \qquad \text{and} \qquad f_\infty^2 h'' = h'' f_\infty.$$

These relations allow us to move f_∞ to the far left of the word, at each step exchanging a power of f_∞ for a power whose absolute value is twice as great, which means we have expressed a as $f_\infty^n(b)$, where $\mathrm{Ind}(b) < \mathrm{Ind}(a)$. Here $|n| = 2^{\mathrm{Ind}(a)-1}$, and the sign of n is determined by the number of 0s among $a_0, \ldots, a_{\mathrm{Ind}(a)-1}$. By induction, we have shown that every point of $\mathfrak{D}$ lies in the union of the orbits of $\bar{0}$ and $1\bar{0}$.

Because $\mathrm{TM}(a)$ is invariant under f_∞, $\bar{0}$ and $1\bar{0}$ are not in the same orbit, and therefore $\mathfrak{D}$ is a disjoint union of these two orbits. ☐

Remark 4.5. It is not hard to show that both f_∞ and F_∞ are ergodic, for example, using elementary linear algebra. It is less clear how the flow in other directions on $(X_\infty, \omega_\infty)$ behaves.

Remark 4.6. We will need a bit more information about the points of discontinuity of f_∞. These correspond precisely to sequences of the form $11\cdots 11\bar{0}$ or $11\cdots 1101\bar{0}$ (the initial number of 1s may be zero). From the information in (3), we see that the forward and backward orbits of both 0 and $1/2$ each contain infinitely many such points.

4.2. **Vertical trajectories and the Veech group of** $(X_\infty, \omega_\infty)$**.**

Lemma 4.7. *Saddle connections are dense in the vertical foliation of* $(X_\infty, \omega_\infty)$*. Every vertical critical trajectory is a saddle connection.*

Proof. Let $x \in \mathfrak{D}$, and consider the point $(x, 0)$ on the boundary of the unit square. If x is not already a point of discontinuity of f_∞, then by Lemma 4.4 and Remark 4.6, there exist $m, n > 0$ such that $f_\infty^{-m}(x)$ and $f_\infty^{n}(x)$ are points of discontinuity of f_∞. Because f_∞ is determined by the vertical flow, this means there is a vertical saddle connection passing through $(x, 0)$ and connecting $(f_\infty^{-m}(x), 0)$ to $(f_\infty^{n}(x), 0)$. If x is a point of discontinuity of f_∞, then so is $f_\infty(x)$, and there is a vertical saddle connection from $(x, 0)$ to $(f_\infty(x), 1)$. $\square$

The proof shows, moreover, that the union of the vertical critical trajectories contains precisely those points that have representatives in Figure 5 with a dyadic rational x-coordinate.

For clarity in the proof of Lemma 4.10, we state the following definition and proposition.

Definition 4.8. An (*open*) *angular sector* is a Riemannian surface isometric to the half-infinite strip

$$U_{t,\Theta} = \{z = x + iy \mid x < \log t,\ 0 < y < \Theta\}$$

with the (conformal) metric $|e^z\,\mathrm{d}z|$. Θ is called the *angle* of the sector, and t is its *radius.*

Proposition 4.9. *Let* (X, ω) *be a translation surface, and let* $\varphi \in \mathrm{Aff}(X, \omega)$ *be an affine homeomorphism. Suppose* X *contains an embedded angular sector* U *whose angle is an integer multiple of* π*. Then* $\varphi(U)$ *contains an angular sector with the same angle as* U*.*

To see why this proposition is true, it suffices to consider the case of a sector with angle π. For then φ transforms the sector into a half-ellipse, which thus contains a sector with angle π and the same center as the ellipse.

Lemma 4.10. *The vertical direction of* $(X_\infty, \omega_\infty)$ *is not affinely equivalent to any other direction on* $(X_\infty, \omega_\infty)$*.*

Proof. Let $\mathcal{F}_v$ be the vertical foliation of $(X_\infty, \omega_\infty)$, and let $\mathcal{F}_\theta$ be the foliation in some other direction θ. Assume there exists some $\varphi \in \mathrm{Aff}(X_\infty, \omega_\infty)$ that sends θ to the vertical direction. Let L be the critical leaf of $\mathcal{F}_\theta$ emanating from $(0, 2/3)$ in Figure 5. Then $\varphi(L)$ must be a critical trajectory in the vertical direction, which means it must be a saddle connection, by Lemma 4.7. By composing φ with some power of ψ_∞ and ρ_∞, if necessary, we may assume $\varphi(L)$ is the saddle connection L_0 from $(0, 0)$ to $(0, 1/2)$.

Now consider an angular sector $U = \mathrm{image}\,(U_{\varepsilon,2\pi} \to X_\infty)$, with $\varepsilon < 1/8$, such that the radius in the direction of angle π is sent to a portion of L_0. By Proposition 4.9, because the angle of U is an integer multiple of π, $\varphi^{-1}(U)$ must also be a sector of angle 2π. But this is impossible, because the two halves of U on either side of L_0 must be sent to sectors of radius π with $\varphi^{-1}(L_0) = L$ as a boundary radius; no such sectors exist, due to the accumulation of saddle connections at $(0, 2/3)$. Therefore no affine homeomorphism can send the vertical direction of $(X_\infty, \omega_\infty)$ to any other direction. $\square$

Remark 4.11. The distinction between vertical critical trajectories on $(X_\infty, \omega_\infty)$ and those emanating from the points $(1/2, 1/3)$ and $(0, 2/3)$ in Figure 5 can also be made using a purely topological criterion, rather than the geometric criterion of Proposition 4.9. This amounts to a study of the space of critical trajectories on a translation surface of infinite type, which is the subject of [BV].

Now we are ready to prove the main theorem of this section.

Proof of Theorem 4.1. By Lemma 4.10, any affine homeomorphism φ of $(X_\infty, \omega_\infty)$ must preserve the vertical direction. Because it must preserve the set of saddle connections, and the lengths of the vertical saddle connections are all powers of 2, the derivative of φ must act on the vertical direction by multiplication by $\pm 2^n$ for some $n \in \mathbb{Z}$. By composing φ with a power of ψ_∞ and ρ_∞, if necessary, we may assume that φ is orientation-preserving and the derivative of φ is the identity in the vertical direction. Note that, because the area of $(X_\infty, \omega_\infty)$ is finite, the derivative of φ must lie in $\mathrm{SL}_2(\mathbb{R})$, which implies that its only eigenvalue is 1.

Thus φ is either a translation automorphism or a parabolic map. The latter is impossible because $(X_\infty, \omega_\infty)$ does not have any cylinders in the vertical direction. The existence of non-trivial translation automorphisms is ruled out directly, for example by observing that each vertical saddle connection has only one other of the same length (its image by ρ_∞), and no translation automorphism can carry one to the other. Therefore the original map φ was a product of a power of ψ_∞ and ρ_∞, and the result is proved. $\square$

Remark 4.12. In the proof of Theorem 4.1, we showed that $(X_\infty, \omega_\infty)$ has no non-trivial translation automorphisms. The same is true of the finite-genus surfaces (X_g, ω_g): as observed in the proof of Corollary 2.6, each (X_g, ω_g) (with $g \geq 4$) has a saddle connection such that no other saddle connection has the same developing vector; this rules out the possibility of $\mathrm{Aff}(X_g, \omega_g)$ containing a non-trivial translation. A similar argument works for $g = 3$. We conclude that for any $3 \leq g \leq \infty$, every affine map of (X_g, ω_g) is uniquely determined by its derivative; this means that $\mathrm{Aff}(X_g, \omega_g)$ can be identified with the Veech group $\Gamma(X_g, \omega_g)$ in $\mathrm{GL}_2(\mathbb{R})$. We can thus compare the groups $\mathrm{Aff}(X_g, \omega_g)$ as subgroups of $\mathrm{GL}_2(\mathbb{R})$, even though *a priori* they are groups of homeomorphisms of surfaces with different genera.

Recall that a sequence $\{\Gamma_n\}_{n=0}^\infty$ of closed subgroups of $\mathrm{GL}_2(\mathbb{R})$ *converges geometrically* to $\Gamma_\infty \subset \mathrm{GL}_2(\mathbb{R})$ if both of the following hold:

(1) If $\{\gamma_n \in \Gamma_n\}$ is a sequence of elements converging to $\lim \gamma_n = \gamma_\infty$, then $\gamma_\infty \in \Gamma_\infty$.
(2) Any $\gamma \in \Gamma_\infty$ is obtained as a limit of $\gamma_n \in \Gamma_n$ as in (1).

It follows immediately from the definitions and from Lemma 2.1 that the sequence $\langle \psi_g, \rho_g \rangle \subset \mathrm{Aff}(X_g, \omega_g)$ converges geometrically to $\langle \psi_\infty, \rho_\infty \rangle = \mathrm{Aff}(X_\infty, \omega_\infty)$. A natural question is whether the groups $\mathrm{Aff}(X_g, \omega_g)$ with g finite converge geometrically to $\mathrm{Aff}(X_\infty, \omega_\infty)$. This question is of particular interest since it is currently unknown whether there exists a translation surface of finite genus whose affine group contains a finite-index cyclic subgroup generated by a pseudo-Anosov element. If it is true that $\mathrm{Aff}(X_g, \omega_g)$ converges to $\mathrm{Aff}(X_\infty, \omega_\infty)$, then this would at least show that the Veech groups of (X_g, ω_g) for g large enough are "close to" cyclic groups.

This result is not yet known, although early investigations with other families of surfaces that converge (uniformly on compact subsets) to a limit surface suggest that one can in general expect the geometric limit of the Veech groups to be contained in the Veech group of the limiting surface. In the case of the Arnoux–Yoccoz surfaces, since we have subgroups of $\mathrm{Aff}(X_g, \omega_g)$ converging to $\mathrm{Aff}(X_\infty, \omega_\infty)$, we would then in fact have the equality $\lim_{n\to\infty} \mathrm{Aff}(X_g, \omega_g) = \mathrm{Aff}(X_\infty, \omega_\infty)$, taking the geometric limit.

Appendix. From the top: $g = 1, 2$

In §3, we extended the family of Arnoux–Yoccoz surfaces (X_g, ω_g) to the index $g = \infty$. In this appendix we extend the construction of §2.2 to create (X_1, ω_1) and (X_2, ω_2) so that the sequence (X_g, ω_g) is defined for all indices $1 \le g \le \infty$.

$g = 1$**.** The defining equation for α in this case is $\alpha = 1$. The corresponding surface is a torus, formed from the unit square by the usual top-bottom and left-right identifications. Hence $(X_1, \omega_1) = (\mathbb{C}/(\mathbb{Z} \oplus i\mathbb{Z}), \mathrm{d}z)$ and ψ_1 is the identity map.

$g = 2$**.** Here we get the defining equation $\alpha^2 + \alpha = 1$, which means that $\alpha = (\sqrt{5} - 1)/2$ is the inverse of the golden ratio, as mentioned in the introduction. Beginning with the unit square, a single square of side length $1 - \alpha = \alpha^2$ is removed from the upper right corner. Two slits are made, one from $(\alpha/2, 0)$ to $(\alpha/2, 1)$ and the other from $((1 + \alpha)/2, 0)$ to $((1 + \alpha)/2, \alpha)$, thereby cutting the staircase into three separate pieces. After the usual identifications are made, following the procedure of §2.2, the result is a disconnected pair of tori. This is to be expected: the corresponding interval exchange map f_2 is reducible. Viewed on the circle $[0, 1]/\{0 \sim 1\}$, it splits into two interval exchanges, each of which swaps a pair of segments whose lengths are in the golden ratio. The pair of tori taken together admits a pseudo-Anosov homeomorphism ψ_2 with expansion constant $1/\alpha = (1 + \sqrt{5})/2$, which in the process exchanges the components.

Genus 2 is not entirely absent in this picture, however. Indeed, the surface constructed above is a limit of surfaces in $\mathcal{H}(1, 1)$ and therefore lies in the principal boundary of this stratum. If we shorten the height of the first slit in the paragraph above to $1 - \varepsilon$ and that of the second slit to $\alpha - \varepsilon$, then the same identifications are possible, and we obtain a connected sum of the two tori, resulting in two cone points of angle 4π. As $\varepsilon \to 0$, the two cone points collapse into a single point, which becomes a marked point on each of the two tori.

Moreover, the period lattices of the two tori that compose X_2 satisfy a remarkable property: if either is scaled by a factor of $\sqrt{5}$, the result is a sublattice of index 5 in the other. This implies that (X_2, ω_2) lies in the boundary of the "eigenform locus" defined by McMullen [Mc] (see also [Ca, §6]), which is composed of surfaces (X, ω) in $\mathcal{H}(1, 1)$ such that the Jacobian variety of X admits real multiplication with ω as an eigenform. (The author thanks Barak Weiss for pointing out this feature of (X_2, ω_2).)

Because (X_2, ω_2) is not connected, we adopt the convention that the group $\mathrm{Aff}(X_2, \omega_2)$ only consists of affine self-maps each of which has constant derivative. The orientation-reversing map $\rho_2 \in \mathrm{Aff}(X_2, \omega_2)$ exchanges the components. By composing any $\varphi \in \mathrm{Aff}(X_2, \omega_2)$ with ρ_2 or ψ_2, if necessary, we may assume that φ is orientation-preserving and also preserves the components of X_2. The orientation-preserving affine group of a torus with a marked point is $\mathrm{SL}_2(\mathbb{Z})$; as was the case in Remark 4.12, the derivative homomorphism is an isomorphism. Thus, to compute the remainder of $\mathrm{Aff}(X_2, \omega_2)$, we wish to find the intersection of the affine groups of the two components. Set

$$M_1 = \begin{pmatrix} 1 & -\alpha \\ \alpha & 1 \end{pmatrix} \qquad \text{and} \qquad M_2 = \begin{pmatrix} \alpha & -1 \\ 1 & \alpha \end{pmatrix}.$$

Following a certain normalization, the two components of X_2 have the columns of M_1 and M_2 for their respective homology bases. Then we want to determine

$$(M_1 \cdot \mathrm{SL}_2(\mathbb{Z}) \cdot M_1^{-1}) \cap (M_2 \cdot \mathrm{SL}_2(\mathbb{Z}) \cdot M_2^{-1})$$

or, equivalently, $(M_2^{-1}M_1 \cdot \mathrm{SL}_2(\mathbb{Z}) \cdot M_1^{-1}M_2) \cap \mathrm{SL}_2(\mathbb{Z})$. We have

$$M_1^{-1}M_2 = (M_2^{-1}M_1)^\top = \frac{\alpha}{2-\alpha}\begin{pmatrix} 2 & -1 \\ 1 & 2 \end{pmatrix}$$

and so we want to find the quadruples of integers (X, Y, Z, W) with $XW - YZ = 1$ such that the following is in $\mathrm{SL}_2(\mathbb{Z})$:

$$M_2^{-1}M_1 \begin{pmatrix} X & Y \\ Z & W \end{pmatrix} M_1^{-1}M_2 = \frac{1}{5}\begin{pmatrix} 4X + 2(Y+Z) + W & 4Y + 2(W-X) - Z \\ 4Z + 2(W-X) - Y & 4W - 2(Y+Z) + X \end{pmatrix}.$$

That is, each of the entries in the final matrix must be congruent to 0 modulo 5. This is a necessary and sufficient condition. All four entries yield the same linear condition $X + 3Y + 3Z + 4W \equiv 0 \bmod 5$, which is satisfied in particular if $X \equiv W \equiv 1$ and $Y \equiv Z \equiv 0 \bmod 5$. Hence the Veech group of (X_2, ω_2) contains a copy of the principle 5-congruence subgroup of $\mathrm{SL}_2(\mathbb{Z})$; it is therefore a lattice in $\mathrm{SL}_2(\mathbb{R})$.

References

[Ar] Pierre Arnoux. Un exemple de semi-conjugaison entre un échange d'intervalles et une translation sur le tore. *Bull. Soc. Math. France* **116**(1988), 489–500 (1989).

[AY] Pierre Arnoux and Jean-Christophe Yoccoz. Construction de difféomorphismes pseudo-Anosov. *C. R. Acad. Sc. Paris Sr. I Math.* **292**(1981), 75–78.

[Bo] Joshua P. Bowman. Orientation-reversing involutions of the genus 3 Arnoux–Yoccoz surface and related surfaces. In *In the tradition of Ahlfors-Bers. V*, volume 510 of *Contemp. Math.*, pages 13–23. Amer. Math. Soc., Providence, RI, 2010.

[BV] Joshua P. Bowman and Ferran Valdez. Isolated singularities of infinite-genus translation surfaces. In preparation.

[Ca] Kariane Calta. Veech surfaces and complete periodicity in genus two. *J. Amer. Math. Soc.* **17**(2004), 871–908.

[Ch] Reza Chamanara. Affine automorphism groups of surfaces of infinite type. In *In the tradition of Ahlfors and Bers, III*, volume 355 of *Contemp. Math.*, pages 123–145. Amer. Math. Soc., Providence, RI, 2004.

[CGL] Reza Chamanara, Frederick P. Gardiner, and Nikola Lakic. A hyperelliptic realization of the horseshoe and baker maps. *Ergodic Theory Dynam. Systems* **26**(2006), 1749–1768.

[EG] Clifford J. Earle and Frederick P. Gardiner. Teichmüller disks and Veech's $\mathcal{F}$-structures. *Contemp. Math.* **201**(1997), 165–189.

[Ha] Allen Hatcher. *Algebraic topology.* Cambridge University Press, Cambridge, 2002.

[Hoo] W. Patrick Hooper. Dynamics on an infinite surface with the lattice property. arxiv:0802.0189v1.

[HHW] W. Patrick Hooper, Pascal Hubert, and Barak Weiss. Dynamics on the infinite staircase. http://www.math.bgu.ac.il/∼barakw/papers/staircase.pdf.

[HL] Pascal Hubert and Erwan Lanneau. Veech groups without parabolic elements. *Duke Math. J.* **133**(2006), 335–346.

[HLM] Pascal Hubert, Erwan Lanneau, and Martin Möller. The Arnoux–Yoccoz Teichmüller disc. *Geom. Funct. Anal.* **18**(2009), 1988–2016.

[HLT] Pascal Hubert, Samuel Lelièvre, and Serge Troubetskoy. The Ehrenfest wind-tree model: periodic directions, recurrence, diffusion. http://hal.archives-ouvertes.fr/docs/00/44/12/12/PDF/windtree.pdf.

[K] Irwin Kra. On the Nielsen–Thurston–Bers type of some self-maps of Riemann surfaces. *Acta Math.* **146**(1981), 231–270.

[Mc] Curtis T. McMullen. Dynamics of $\mathrm{SL}_2(\mathbb{R})$ over moduli space in genus two. *Ann. Math. (2)* **165**(2007), 397–456.

[PSV] Piotr Przytycki, Gabriela Schmithüsen, and Ferran Valdez. Veech groups of Loch Ness monsters. To appear in *Annales de l'Institut Fourier*, currently at arXiv:math/0906.5268v1.

[Th] William P. Thurston. On the geometry and dynamics of diffeomorphisms of surfaces. *Bull. A.M.S.* **19**(1988), 417–431.

[Ve] William A. Veech. Teichmüller curves in moduli space, Eisenstein series, and an application to triangular billiards. *Inv. Math.* **97**(1989), 553–583.

Institute of Mathematical Sciences, Stony Brook University, Stony Brook, NY 11794